Supporting Information

Elemental and Morphological Diversity of Individual Magnetic Particles from Urban Surfaces: Implications for Adverse Health Outcomes

Xiangxing Long,[1, 2 #] Jonas Wielinski,[3 #] Zhe Zhao,[1] * Pierre Herckes,[4] Manuel A Roldan,[5] Gregory V. Lowry,[3] and Paul Westerhoff [1]

[1] Nanosystems Engineering Research Center for Nanotechnology-Enabled Water Treatment, School of Sustainable Engineering and the Built Environment, Arizona State University, Tempe, Arizona 85287-3005, United States

[2] Biodesign Swette Center for Environmental Biotechnology, Arizona State University, Tempe, Arizona 85287-3005, United States

[3] Department of Civil and Environmental Engineering, Carnegie Mellon University, Pittsburgh, Pennsylvania 15213, United States

[4] School of Molecular Sciences, Arizona State University, Tempe, Arizona 85287-1604, United States

[5] Eyring Materials Center, Arizona State University, Tempe AZ 85287-3005, USA

[#] These authors contribute equally to this study.

* Corresponding Author: Zhe Zhao; Email: zzhao146@asu.edu ; Phone: 619-375-9855; orcid ID: 0000-0003-2848-9058-000

Text S1

For the collection of magnetic materials from parking garage surfaces, an industrial grade Neodymium N48 magnetic bar (3 x 1/2 x 1/8 Inch; totalElement, Centennial, CO) coated with Teflon Parafilm was mounted on a rod. Magnetic dust was collected by gently rubbing and passing the magnet on the ground surface (Figure S1). The collected material was removed from the Parafilm covering the magnet, combined, and then gently rubbed with an agate mortar and pestle. We collected magnetic dust from parking structures, including both parking areas and driveways. The collected dust was then sieved using a commercial sieve (53 μm nylon mesh sieve, Bel-Art, Wayne, NJ). Beneath this nylon mesh another Neodymium N48 magnet, wrapped in weighing paper and a layer of parafilm, was positioned to effectively draw MDPs through the sieve. This procedure facilitated separation of almost exclusively MDPs in our samples rather than capturing all particles. We only considered inhalable particles in this work. We utilized Parafilm and weighing paper to prevent any direct contact between the Neodymium magnet and the MDPs, ensuring the integrity of our samples. Some of the original dust included large solid materials (e.g., nails, plastic fragments, and concrete residue) that were captured by the magnet but could not pass through the sieve, and were therefore excluded from analysis as they were not considered to be of inhalable size. Magnetically captured particles often adhered to or were entangled with larger debris. Gently rubbing the material with a pestle helped to dislodge the magnetic particles from the non-magnetic trash. Subsequent magnet-facilitated sieving further aided in removing non-magnetic debris and refining the magnetic dust particles (MDPs) used in this study. The final mass of sieved MDPs was approximately 20 mg and was processed for subsequent material characterizations.

Text S2

The spICP-TOFMS instrument was tuned daily with a 1 ppb solution of Co, In, Ce, and U. The oxide ratio, measured as $^{140}Ce^{16}O/^{140}Ce$, remained below 2.5%, and the resolving power was approximately 3000 during all experimental runs. A peristaltic pump mounted to the front end of the icpTOF R facilitated sample introduction. An aerosol was generated inside a cooled (4°C) cyclonic spray chamber using a MicroMist nebulizer, which was then directed into a 2.5 mm injector set to a 5 mm sampling depth. Sample data were acquired for 360 s with a 2 ms dwell time, while dissolved standard data for external calibration were obtained for 60 s with a 1 s dwell time. Isotopes ranging from ^{28}Si to ^{238}U were recorded and calibrated. Particle events were differentiated from the dissolved background using the following example formula: $Threshold = \mu + 3.29\sigma + 2.72$.[1-3] In this formula, μ represents the mean and σ the standard deviation of the instrument-recorded intensity, determined within a window of 100 dwell times. Values exceeding the threshold were considered particle events, and intensities were converted to mass/particle based on an algorithm from a previous study.[4] To assess transport efficiency, 40 nm Au nanoparticles were recorded.

Text S3

EDX elemental atomic percentage data were used directly for HCA particle classification. Particles of similar elemental composition were grouped together, which might yield particle groups such as crust-related metal oxides, iron oxides or metallic iron. Although elemental similarity was used as the only criteria for particle classification, potential differences in particle morphology were also discussed based on STEM imaging. A student's t-test was conducted to assess the statistical significance of differences in particle morphology between particle groups.

spICP-TOFMS data requires a special treatment in particle classification different from EDX data due to the different data structure. The exclusion of oxygen and difference in elemental

absolute weight in spICP-TOFMS maximize the difference between particles, and so we need additional data processing for the spICP-TOFMS in particle classification. The absolute weight of each element on the analyzed particle might vary at several magnitudes (e.g., ~1 to 5 magnitudes for Fe in the MDPs). To minimize the bias caused by difference in absolute weight of different particles, the absolute weight of each element detected on each particle was normalized to the maximum weight of the same element among all detected particles. Based on the normalized mass, particles characterized by spICP-TOFMS were classified into a certain number of groups based on elemental similarity, ensuring that the largest group contained less than 10% of particles and so the difference observed among >90% particles were considered in HCA particle classification. If we assigned very few particle groups (<10 particle groups) in total for spICP-TOFMS, only the largest mathematical difference can be considered in HCA and >95% particles were assigned into one group, but these >95% particles can still be chemically different. After HCA classification, further manual classification was required to merge similar particle groups based on a previous study, because mathematically different groups/clusters may still be similar from a chemical perspective.[5] The justification for this additional manual merging is the authors' knowledge about what distinction between particles is important for a study.[5] If two particle groups displayed similar elemental composition, this study no longer considered any difference in their normalized elemental absolute weight. For example, if Al is the only element detected in spICP-TOFMS for two particle groups, these two particle groups will be merged although they might be 1~2 magnitude different in the normalized absolute mass of Al.

Table S1 Elemental composition of digested magnetic dust particles measured by ICP-MS

Element	Mass concentration (mg/g)
Fe	735 ± 6
Ti	9.2 ± 0.2
Mn	4.44 ± 0.04
Al	2.8 ± 0.07
Mg	1.5 ± 0.03
Cr	1.30 ± 0.01
Cu	1.27 ± 0.02
Zn	0.93 ± 0.02
V	0.61 ± 0.01
Ni	0.414 ± 0.004
Ba	0.195 ± 0.002
Sr	0.178 ± 0.004
Mo	0.115 ± 0.003
Co	0.111 ± 0.001
Sb	0.0297 ± 0.0006
Zr	0.0161 ± 0.003
Nd	0.0158 ± 0.0002
Pb	0.0120 ± 0.0003
Pr	0.00449 ± 0.00007

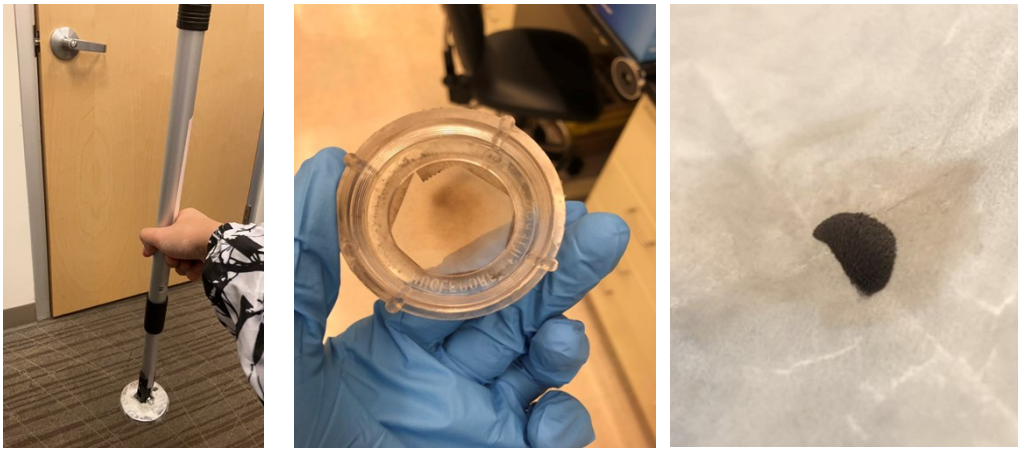

Figure S1. Photographs (from left to right) of magnetic bar on end of sampling rod, nylon filter and sieved magnetic dust

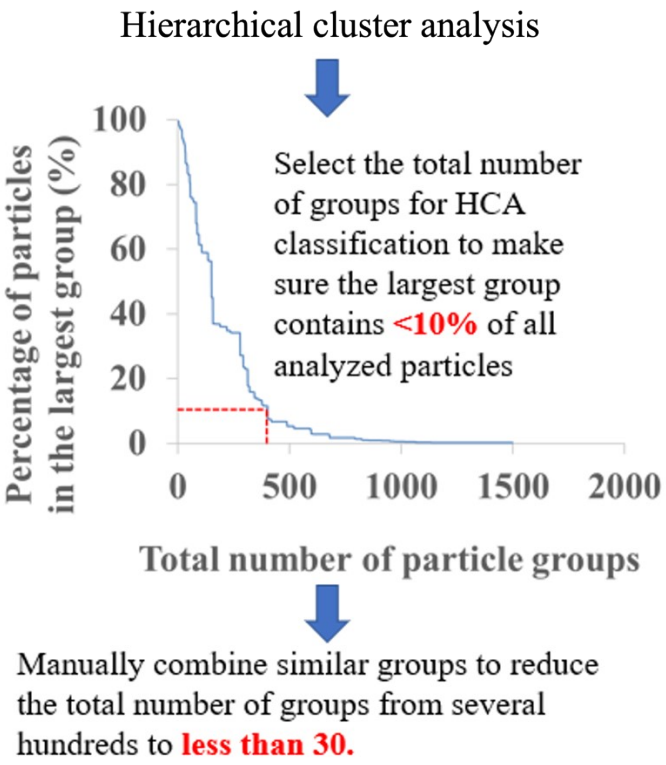

Figure S2. Particle classification for spICP-TOFMS results. The particles were first classified into hundreds of groups to ensure the largest group contained less than 10% of the analyzed particles. Manual classification was adopted to combine similar groups, reducing the total number of groups from several hundred to less than 30.

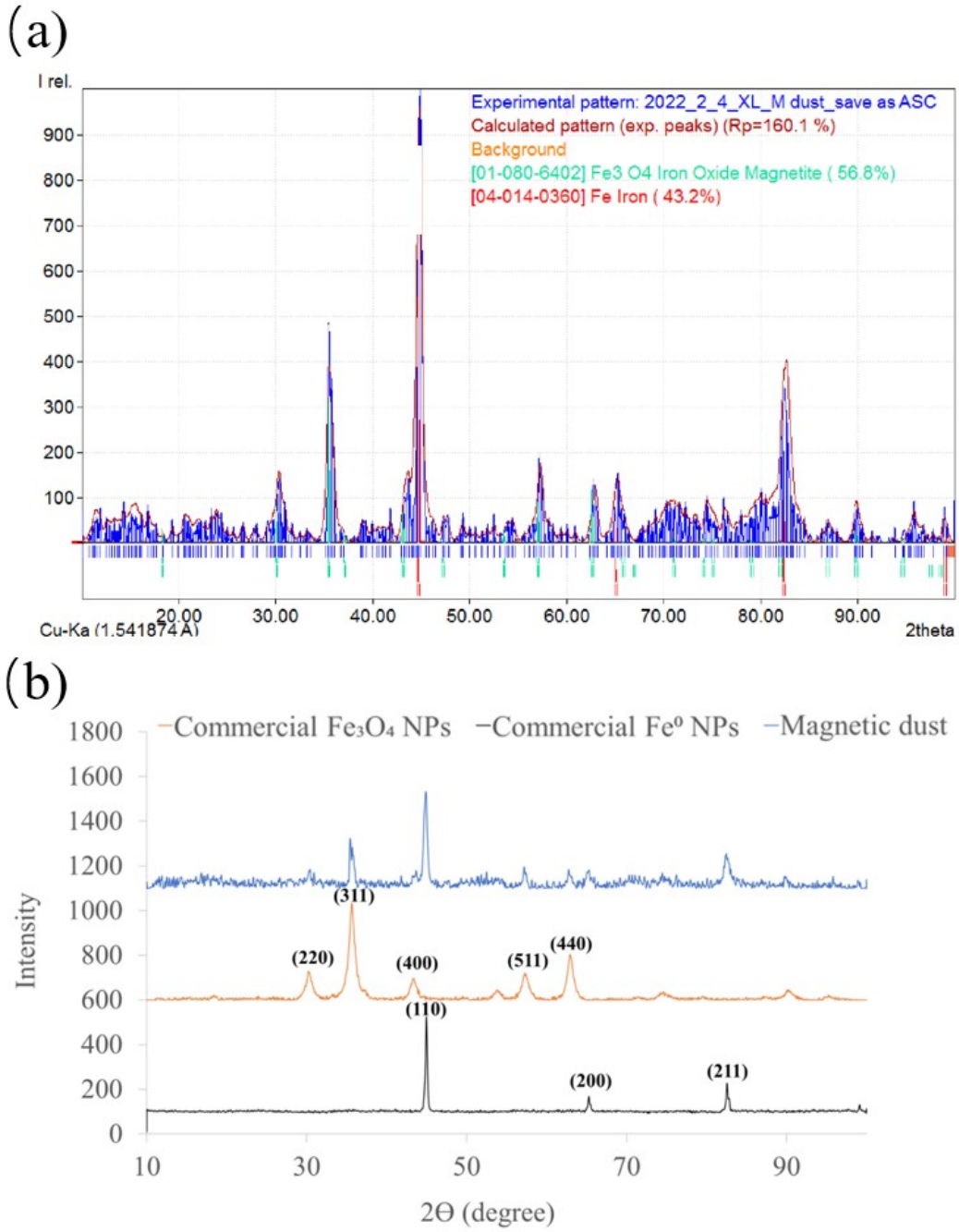

Figure S3. XRD analysis of MDPs. a) XRD elemental estimation of magnetic dust using Match! 2 software. The magnetic dust particles contain approximately 43% elemental iron and 57% magnetite. b) XRD pattern of magnetic dust (blue curve), magnetite (orange curve) and metallic iron nanoparticles (black curve). The crystal surface of Fe_3O_4 and Fe^0 corresponding to each mineral was labeled above its XRD peak.

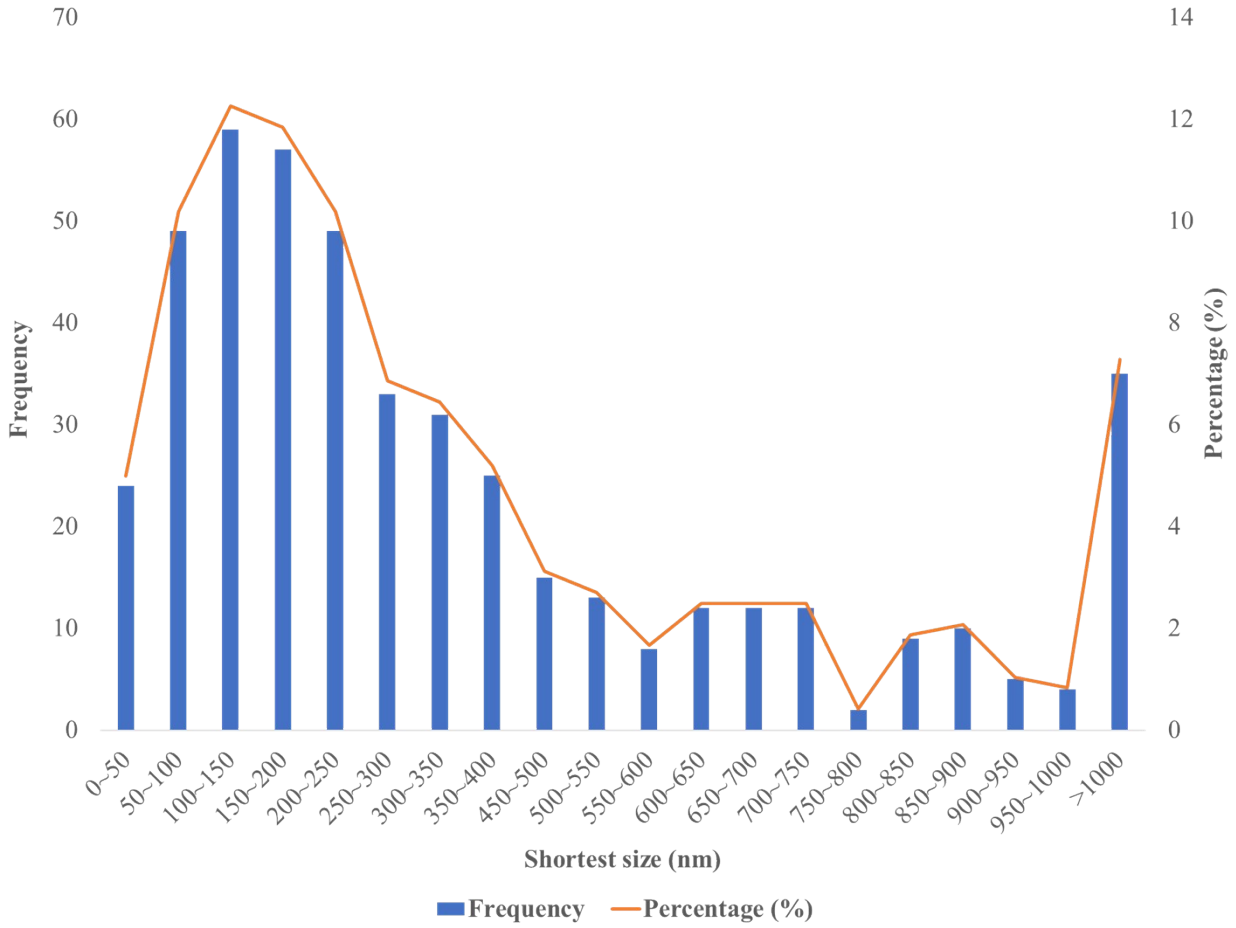

Figure S4. Particle size distribution pattern of 481 particles based on the shortest diagonal measured by STEM imaging.

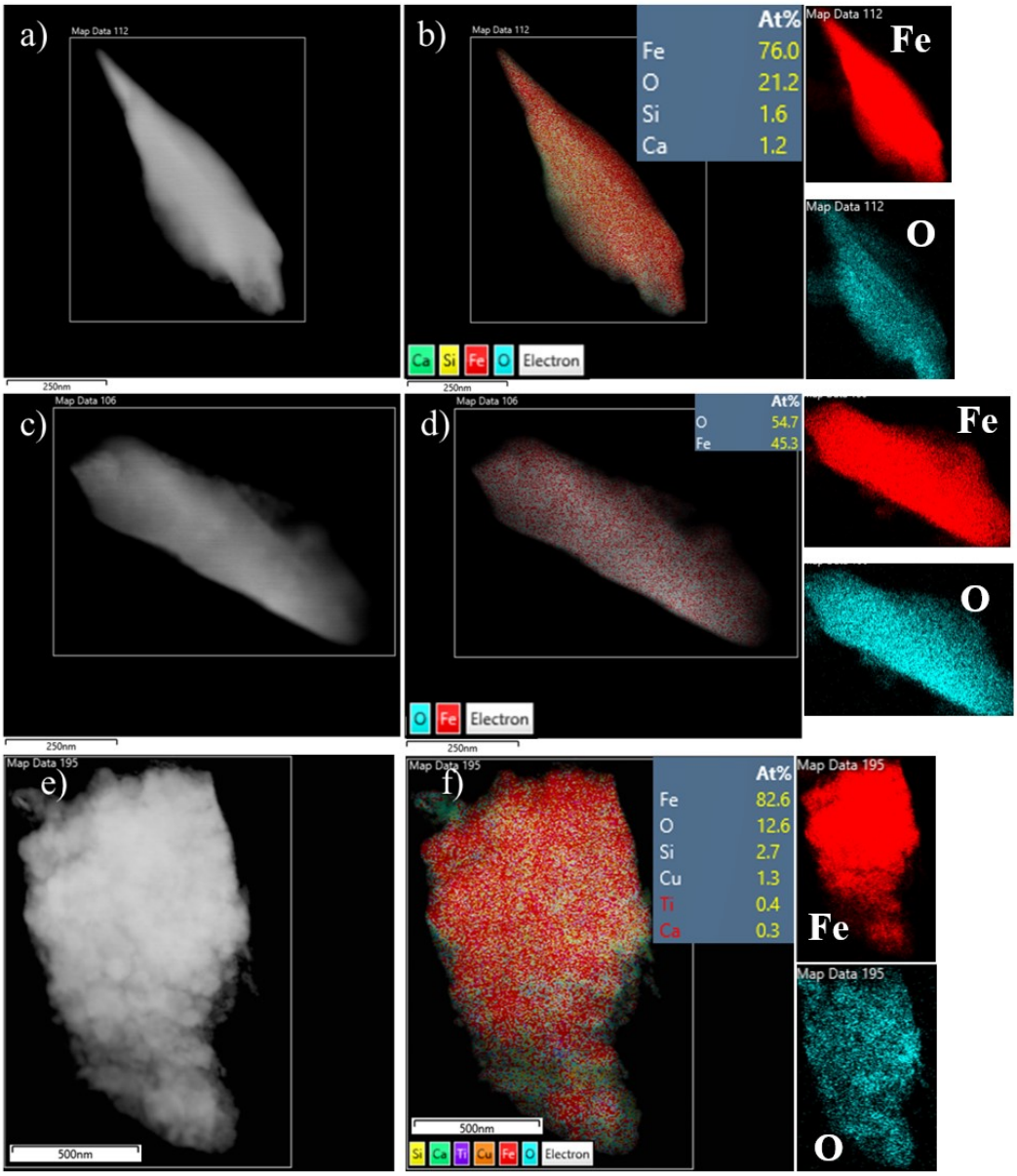

Figure S5 STEM-EDX analysis of magnetic dust particles. a) is an elongated metallic iron particle, with EDX mapping and elemental quantification shown in b). c) is an iron oxide particle, with EDX mapping and elemental quantification shown in d). e) is a metallic iron particle enriched with Si, Cu, Ti, and Ca, quantified by EDX in f). Fe and O maps are included adjacent to the EDX elemental analysis in b), d), and f).

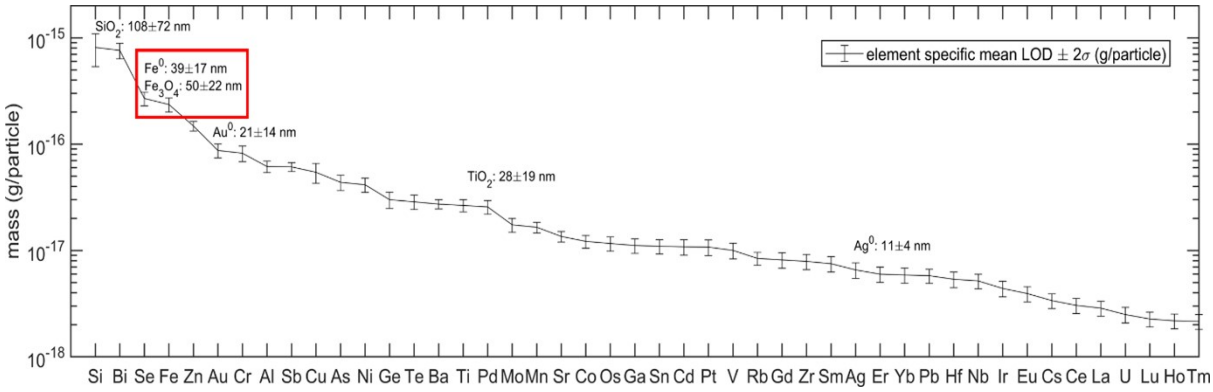

Figure S6 spICP-TOFMS particle mass limits in grams per particle from the highest limit of detection (LOD) (Si) to the lowest (Tm). The detection limit is calculated using the formula: Threshold = $\mu + 3.29\sigma + 2.72$, where μ represents the mean and σ the standard deviation of the instrument-recorded intensity, determined within a window of 100 dwell times. In this graph, the mean value corresponds to the mean LOD across all measurements of this study, and the error bars indicate $\pm 2\sigma$. Size equivalents of typically encountered mineralogical phases were calculated for selected elements (Si, Fe, Au, Ti, and Ag).

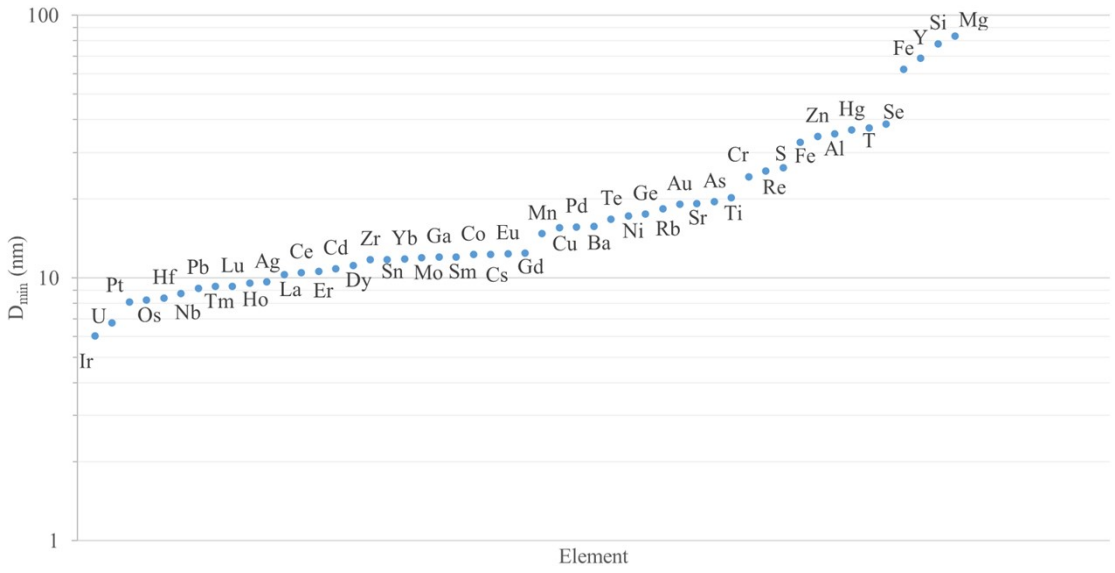

Figure S7. spICP-TOFMS particle size detection limits (D_{min}) for elements detected in this study. The detection limit is calculated by the: threshold = $\mu + 3.29\sigma + 2.72$, where μ represents the mean and σ the standard deviation of the instrument-recorded intensity, determined within a window of 100 dwell times. Calculations assumed particles were pure in elemental composition and spherical in shape.

References

(1) Tanner, M.; Günther, D. Short transient signals, a challenge for inductively coupled plasma mass spectrometry, a review. *Analytica Chimica Acta* **2009**, *633*, 19-28.

(2) Bland, G. D.; Battifarano, M.; Pradas Del Real, A. E.; Sarret, G.; Lowry, G. V. Distinguishing Engineered TiO(2) Nanomaterials from Natural Ti Nanomaterials in Soil Using spICP-TOFMS and Machine Learning. *Environ Sci Technol* **2022**, *56*, 2990-3001.

(3) Bland, G. D.; Zhang, P.; Valsami-Jones, E.; Lowry, G. V. Application of Isotopically Labeled Engineered Nanomaterials for Detection and Quantification in Soils via Single-Particle Inductively Coupled Plasma Time-of-Flight Mass Spectrometry. *Environmental Science & Technology* **2022**, *56*, 15584-15593.

(4) Pace, H. E.; Rogers, N. J.; Jarolimek, C.; Coleman, V. A.; Higgins, C. P.; Ranville, J. F. Determining Transport Efficiency for the Purpose of Counting and Sizing Nanoparticles via Single Particle Inductively Coupled Plasma Mass Spectrometry. *Analytical Chemistry* **2011**, *83*, 9361-9369.

(5) Murphy, D. M.; Middlebrook, A. M.; Warshawsky, M. Cluster Analysis of Data from the Particle Analysis by Laser Mass Spectrometry (PALMS) Instrument. *Aerosol Science and Technology* **2003**, *37*, 382-391.